

Interacting Dirac Fermions on a Topological Insulator in a Magnetic Field

Vadim M. Apalkov

Department of Physics and Astronomy, Georgia State University, Atlanta, Georgia 30303, USA

Tapash Chakraborty[†]

Department of Physics and Astronomy, University of Manitoba, Winnipeg, Canada R3T 2N2

(Dated: November 8, 2018)

We have studied the fractional quantum Hall states on the surface of a topological insulator thin film in an external magnetic field, where the Dirac fermion nature of the charge carriers have been experimentally established only recently. Our studies indicate that the fractional quantum Hall states should indeed be observable in the surface Landau levels of a topological insulator. The strength of the effect will however be different, compared to that in graphene, due to the finite thickness of the topological insulator film and due to the admixture of Landau levels of the two surfaces of the film. At a small film thickness, that mixture results in a strongly non-monotonic dependence of the excitation gap on the film thickness. At a large enough thickness of the film, the excitation gap in the lowest two Landau levels are comparable in strength.

In recent years, there has been an upsurge of interest on the unusual magnetic properties of Dirac fermions in condensed matter systems. Graphene [2, 3] is one such system where those properties were exhaustively investigated theoretically [4] and experimentally [5, 6]. The most remarkable of those are the existence of a Landau level at zero energy having no magnetic field dependence, and the square root dependence of higher energies on the Landau level (LL) index and the magnetic field [5, 6]. A direct consequence of these is the unusual half-integer quantum Hall effect (QHE). The role of Coulomb interactions between Dirac fermions in graphene, in the fractional QHE (FQHE) regime, was first studied by us theoretically [7]. The effect was later observed in the experiments [8, 9].

Linear dispersion relation in the band structure of massless Dirac fermions, first observed in monolayer graphene [2, 3, 10], is also expected to be present in special insulators with topologically protected surface states [11, 12]. The surface states in these topological insulators (TIs) are gapless with linear relativistic dispersion relation, and therefore bear a close analogy, albeit with some major differences [13], to the energy spectra in graphene. In an external magnetic field, the energetics of the surface Landau levels in the TIs is also similar to that of the Landau levels in graphene. Recently, a direct observation of Landau quantization in a TI, $\text{Bi}_{1-x}\text{Sb}_x$ thin film, was reported, which was found to have the same behavior as in graphene, but are found to be suppressed by surface impurities, thereby indicating its two-dimensional (2D) nature [14, 15]. Although the low-energy dynamics of the surface states is similar to that of graphene, there is an important difference between these two systems. While the electronic states in graphene are strictly two-dimensional and localized within a single graphene layer, the surface states of a TI have finite width in the growth direction. This modifies the inter-electron interaction potential and changes the properties of the FQHE states. In traditional non-relativistic electron systems, an increase in width of the 2D layer results in a reduction

of the FQHE gaps, which in turn reduces the stability of the corresponding incompressible states [16]. Therefore, we should expect that the FQHE gaps in the TIs are also influenced by the finite width, in contrast to the case in graphene. Experimental observation of the Landau quantized topological surface states, in particular the field-independent LL at the Dirac point [14, 15], the signature effect of Dirac fermions, has paved the way for future observation of the QHE in the surface states of the TI. The nature of the FQH states in such a system is the subject of this Letter.

To analyze the properties of the FQHE in the surface states of the TIs, we begin with the low-energy effective Hamiltonian already introduced in the literature [17, 18]. The Hamiltonian has the matrix form of size 4×4 and is given by

$$\mathcal{H}_{\text{TI}} = \epsilon(\vec{p}) + \begin{pmatrix} M(\vec{p})\sigma_z + A_1 p_z \sigma_x & A_2 p_- \sigma_x \\ A_2 p_+ \sigma_x & M(\vec{p})\sigma_z - A_1 p_z \sigma_x \end{pmatrix}, \quad (1)$$

where σ_i are the Pauli matrices, $\epsilon(\vec{p}) = C_1 + D_1 p_z^2 + D_2(p_x^2 + p_y^2)$, $M(\vec{p}) = M_0 - B_1 p_z^2 - B_2(p_x^2 + p_y^2)$. Here we consider a prototypical TI, Bi_2Se_3 , with one surface state containing a single isotropic Dirac cone at the center of the Brillouin zone. For this system the constants are [18], $A_1 = 2.2 \text{ eV}\cdot\text{\AA}$, $A_2 = 4.1 \text{ eV}\cdot\text{\AA}$, $B_1 = 10 \text{ eV}\cdot\text{\AA}^2$, $B_2 = 56.6 \text{ eV}\cdot\text{\AA}^2$, $C_1 = -0.0068 \text{ eV}$, $D_1 = 1.3 \text{ eV}\cdot\text{\AA}^2$, $D_2 = 19.6 \text{ eV}\cdot\text{\AA}^2$, and $M_0 = 0.28 \text{ eV}$. The topological insulator film has a finite thickness of L_z , i.e., the two surfaces of the film are at $z = 0$ and $z = L_z$. The four-component wavefunctions corresponding to the Hamiltonian (1) determine the amplitudes of the wavefunctions at the positions of Bi and Se atoms: $(\text{Bi}_\uparrow, \text{Se}_\uparrow, \text{Bi}_\downarrow, \text{Se}_\downarrow)$, where the arrows indicate the direction of the electron spin.

The external magnetic field, B , along the z -direction produces surface Landau levels which can be found from the Hamiltonian matrix by replacing the x and y components of the momentum by the generalized momentum [20] and introducing the Zeeman energy, $\Delta_z = \frac{1}{2}g_s\mu_B B$.

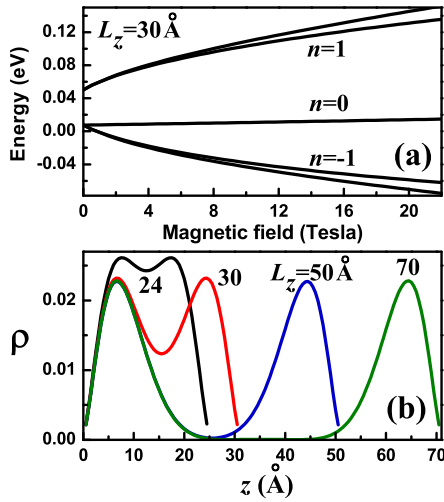


FIG. 1: (a) The lowest surface Landau levels of a TI film shown for the film thickness $L_z = 30$ Å. For each n there are two LLs of the TI film, belonging to two surfaces of the film. (b) The electron density along the z axis for one of the $n = 1$ Landau levels and for different values of the thickness, L_z , of the Bi_2Se_3 film. The numbers next to the lines are the values of L_z . The magnetic field is at 15 Tesla.

Here $g_s \approx 8$ is the effective g -factor of surface states [17, 19] and μ_B is the Bohr magneton. For the surface Landau level n the wavefunctions are of the form

$$\Psi_n^{(\text{TI})} = \begin{pmatrix} \chi_n^{(1)}(z)\phi_{|n|-1,m} \\ \chi_n^{(2)}(z)\phi_{|n|-1,m} \\ i\chi_n^{(3)}(z)\phi_{|n|,m} \\ i\chi_n^{(4)}(z)\phi_{|n|,m} \end{pmatrix}, \quad (2)$$

for $n > 0$. For $n = 0$, the functions $\chi_{n=0}^{(1)}$ and $\chi_{n=0}^{(2)}$ vanish identically. Here $\phi_{n,m}$ are wavefunctions of conventional non-relativistic LLs with index n and some other intra-Landau level index, m , for example, the z component of the angular momentum. The functions $\chi_n^{(i)}(z)$ satisfy the following eigenvalue equation

$$\begin{aligned} \epsilon \hat{\chi}_n(z) = & \begin{pmatrix} \epsilon_{z,n}^{(+)} + M_{z,n}\sigma_z & 0 \\ 0 & \epsilon_{z,n+1}^{(-)} + M_{z,n+1}\sigma_z \end{pmatrix} \hat{\chi}_n(z) \\ & + \begin{pmatrix} iA_1\sigma_x \frac{d}{dz} & -\frac{\sqrt{2(n+1)}}{\ell_0} A_2\sigma_x \\ -\frac{\sqrt{2(n+1)}}{\ell_0} A_2\sigma_x & -iA_1\sigma_x \frac{d}{dz} \end{pmatrix} \hat{\chi}_n(z), \end{aligned} \quad (3)$$

where $\epsilon_{z,n}^{(\pm)} = C_1 + D_2(2n+1)/\ell_0^2 - D_1 \frac{d^2}{dz^2} \pm \Delta_z$ and $M_{z,n} = M_0 - B_2(2n+1)/\ell_0^2 - B_1 \frac{d^2}{dz^2}$. Here $\ell_0 = \sqrt{e\hbar/cB}$ is the magnetic length and $\hat{\chi}_n = (\chi_n^{(1)}, \chi_n^{(2)}, \chi_n^{(3)}, \chi_n^{(4)})^T$. The solution of the system of equations (3) determines

the Landau energy spectrum of the system and the width in the z -direction of the Landau level wavefunctions. This width depends on the Landau level index, the strength of the magnetic field, and the thickness of the TI film. Each surface of the TI film has a corresponding set of surface LLs. The LLs of two surfaces of TI are coupled, which is more pronounced for a narrow TI film, $L_z \lesssim 30$ Å. For TI films of large thickness, the LLs of two surfaces can be considered as decoupled. In Fig. 1 we illustrate the properties of the surface LLs, which were obtained from the numerical solution of Eq. (3). In what follows, we consider only the lowest surface LLs with indices $n = 0$ and $n = 1$. Strong FQHEs can be observed only in these LLs. In Fig. 1(a), the LL energy spectrum is shown as a function of the magnetic field, B , for a TI film of thickness $L_z = 30$ Å. The \sqrt{B} -dependence of the energy of $n = 1$ ($n = -1$) LLs is visible, which is a specific property of the relativistic dispersion law of the surface states of the TI. For each value of n there are two degenerate surface LLs, belonging to the two surfaces. The degeneracy of these LLs is lifted due to their coupling. For $n = 0$, the inter-Landau level coupling is relatively weak and the $n = 0$ LL remains almost doubly degenerate. The coupling of the surface LLs is illustrate in Fig. 1(b), where the electron density, $\rho(z) = |\chi_n^{(1)}|^2 + |\chi_n^{(2)}|^2 + |\chi_n^{(3)}|^2 + |\chi_n^{(4)}|^2$, is shown for different thicknesses of the TI film and for one of the $n = 1$ LLs. For a small thickness of the TI film the surface LLs strongly overlap in space, which results in a strong inter-LL coupling and large electron density within the whole TI film. With increasing film thickness the surface LLs become decoupled with strong localization at the surfaces of the TI film and zero electron density in the bulk region of the film.

In the FQHE regime the electrons partially occupy a single LL and the properties of such a system are completely determined by the electron-electron interaction potential within the corresponding LL [16]. The interaction potential projected on a given LL is determined by the Haldane pseudopotentials [21], which are the energies of two electrons with relative angular momentum m . With the known wavefunctions (2) of the LL with index n the pseudopotentials can be readily evaluated.

Just as in graphene, the $n = 0$ Landau level in a TI is identical to the $n = 0$ traditional (non-relativistic) Landau level but with a finite width, while the $n > 0$ LL in the TI is a mixture of the n and $n - 1$ non-relativistic states. In graphene, such a mixture results in the strongest FQHE being in the $n = 1$ LL [7]. Similar behaviour is also expected in a TI film. To study the properties of the FQHE in a TI we numerically evaluate the energy spectrum of a finite N -electron system in the spherical geometry [21]. The radius of the sphere is $\sqrt{S}\ell_0$, where $2S$ is the number of magnetic fluxes through the sphere in units of the flux quantum. For a given number of electrons, the radius of the sphere determines the filling factor of the system. For example, the $\nu = 1/m$ FQHE (m is an odd integer) corresponds to the relation

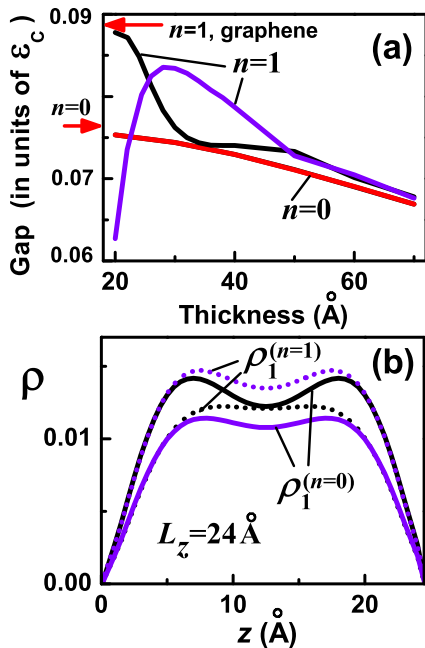


FIG. 2: (a) The $\nu = \frac{1}{3}$ FQHE gap, shown for different Landau levels of a TI film as a function of the film thickness. The magnetic field is 15 Tesla. The excitation gaps were obtained numerically for a finite-size system of $N = 9$ electrons and the parameter of the sphere $S = 12$ [21]. The energy is shown in units of the Coulomb energy, $\varepsilon_C = e^2/\kappa\ell_0$. The red arrow indicates the FQHE gap in the $n = 0$ Landau level of graphene. (b) The electron densities $\rho_1^{(n=1)}(z)$ and $\rho_1^{(n=0)}(z)$ of two $n = 1$ Landau levels at a film thickness of $L_z = 24 \text{ \AA}$. The black (solid and dotted) lines correspond to the $n = 1$ Landau level in panel (a) (black line), while the blue (solid and dotted) lines correspond to the $n = 1$ Landau level in panel (a) (blue line). The densities $\rho_1^{(n=1)}(z) = |\chi_n^{(3)}(z)|^2 + |\chi_n^{(4)}(z)|^2$ and $\rho_1^{(n=0)}(z) = |\chi_n^{(1)}(z)|^2 + |\chi_n^{(2)}(z)|^2$ show the occupations of the $n = 1$ and $n = 0$ non-relativistic Landau level functions, respectively.

$S = (\frac{m}{2})(N - 1)$. The corresponding collective excitation gap determines the stability of the FQHE [16].

The specific properties of the surface LLs in TI films that modify the inter-electron interaction strength within a single LL and change the stability of corresponding FQHE are, (i) the inter-LL coupling of LLs of two surfaces modifies the structure of the corresponding wavefunctions and changes the mixture of the n and $n - 1$ non-relativistic LL functions. This effect is visible only for the $n = 1$ TI Landau level and is the strongest at small thickness of the TI film, for which the inter-LL mixture is strong (see Fig. 1), and (ii) the finite thickness of the TI film results in a finite width of the wavefunctions, which reduces the interaction strength and hence reduces the FQHE gaps.

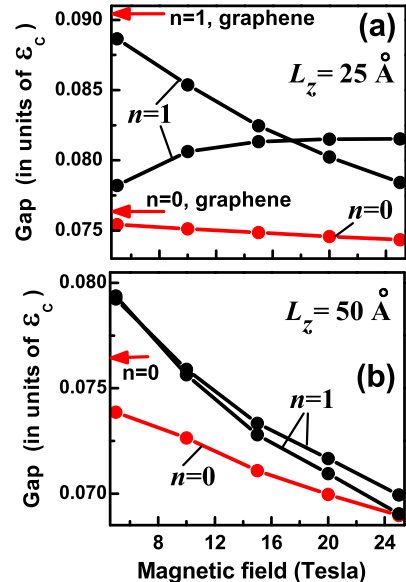


FIG. 3: The $\nu = \frac{1}{3}$ FQHE gap for different Landau levels of the TI film: two $n = 1$ LLs (black lines) and one $n = 0$ LL (red line). The thickness of the film is (a) $L_z = 25 \text{ \AA}$ and (b) $L_z = 50 \text{ \AA}$. The red arrows show the FQHE gaps in the $n = 0$ and $n = 1$ Landau levels of graphene. The FQHE gaps were obtained numerically for a finite-size system of $N = 9$ electrons and the parameter of sphere $S = 12$. The energy is shown in units of the Coulomb energy, $\varepsilon_C = e^2/\kappa\ell_0$.

To illustrate the manifestation of these two effects, we present in Fig. 2 the dependence of the $\nu = \frac{1}{3}$ excitation gap on the thickness of the TI film for $n = 0$ and $n = 1$ LLs and a fixed magnetic field. For large thickness of the TI film (see Fig. 2(a)) the inter-LL coupling is weak and the surface LLs are decoupled. In this case the main effect of the TI film on the FQHE states is through the finite width of the LL wavefunctions, which results in a reduction of the FQHE gaps. The monotonic reduction of the gaps for both $n = 0$ and $n = 1$ TI Landau levels is clearly visible in Fig. 2(a) for large L_z . The corresponding gap in a thicker TI film is usually less than the gap in $n = 0$ LL of graphene (shown by the red arrow in Fig. 2(a)). The reduction is more pronounced for the $n = 1$ LL and for large L_z the gaps in the $n = 1$ and $n = 0$ LLs become comparable. Although the reduction of FQHE in a thick TI film is relatively large, the FQHE should be observable with a larger gap at the $n = 1$ surface LLs.

At a small thickness of the TI film, the inter-LL mixture becomes strong, which modifies considerably the behavior of the FQHE gaps in the $n = 1$ LLs. Since the $n = 0$ TI Landau level consists of the $n = 0$ non-relativistic LL wavefunction, the mixture of surface LLs has a weak effect on the interaction strength and the FQHE gaps in the $n = 0$ LLs. As a result, the FQHE

gap in the $n = 0$ LL monotonically decreases with the TI film thickness within the whole range of L_z due to the finite width of the LL wavefunctions.

The $n = 1$ TI Landau level shows a different behavior. Since the $n = 1$ TI Landau level is a mixture of the $n = 0$ and $n = 1$ non-relativistic LL wavefunctions, the interaction potential becomes sensitive to the inter-LL coupling because such a coupling modifies the contribution of the $n = 0$ and $n = 1$ non-relativistic LL wavefunctions. As a result two $n = 1$ TI Landau levels, although having almost the same energy, show different behavior as a function of L_z . The difference between the two $n = 1$ LLs is illustrated in Fig. 2(b), which shows the contributions of the $n = 0$ and $n = 1$ non-relativistic LL functions to the TI LLs. Clearly, one of the $n = 1$ TI LL (black lines) has a large contribution from the $n = 0$ non-relativistic LL functions, while the other $n = 1$ TI LL (blue line) has a large contribution from the $n = 1$ non-relativistic LL functions. Due to these different contributions the FQHE gap of one of the $n = 1$ LLs is large (almost equal to the gap of $n = 1$ LL in graphene) for small L_z and decreases with increasing thickness of the TI film. The FQHE gap at the other $n = 1$ LL is small at small L_z and with increasing L_z shows a well-pronounced maximum at $L_z \sim 30 \text{ \AA}$ (see Fig. 2(a)).

Another way to see these different properties of small and large thickness of the TI film is to study the dependence of the FQHE gaps on the magnetic field. In Fig. 3 we present the dependence of the $\nu = \frac{1}{3}$ FQHE gap on the magnetic field for two TI films with different thicknesses, $L_z = 25 \text{ \AA}$ (small), and $L_z = 50 \text{ \AA}$ (large). For a large thickness of the TI film, $L_z = 50 \text{ \AA}$ (see Fig. 3(b)) the surface LLs are decoupled. In this case the finite width of the LL wavefunctions results in a monotonic reduction of the FQHE gaps for both $n = 0$ and $n = 1$ LLs. The strength of such a reduction is characterized by the dimensionless width of the LL wavefunctions, expressed in

units of the magnetic length, ℓ_0 . With increasing magnetic field, the magnetic length decreases resulting in an increase of the dimensionless width of the LL wavefunctions.

At a small thickness of the TI film, the inter-LL mixture is strong, which does not affect the FQHE gap in the $n = 0$ LL but modifies the behavior of the FQHE gaps in the $n = 1$ LL. For one of the $n = 1$ LLs the FQHE gap decreases with increasing magnetic field, while for the other $n = 1$ LL the FQHE gap increases with the magnetic field. Such an increase is the direct manifestation of inter-LL coupling. For both $n = 1$ LLs the FQHE gap lies between the FQHE gaps of $n = 0$ and $n = 1$ LLs of graphene.

Therefore, the FQHE can indeed be observed in the surface Landau levels of a topological insulator. The strength of the FQHE, which is characterized by the value of the excitation gap, is however reduced somewhat with increasing thickness of the TI film. This is due to an increase of the width in the z -direction of the surface Landau level wavefunctions. The finite thickness of the TIs notwithstanding, the FQHE gaps are the largest in the $n = 1$ Landau level, which is similar to the case of a monolayer graphene [7]. The reduction of the FQHE gaps is more pronounced in the $n = 1$ Landau level. For the $n = 1$ TI Landau levels the dependence of the FQHE gaps on the thickness of the film is strongly non-monotonic at a small thickness, which is due to strong inter-LL coupling. At a large enough thickness of the film, $L_z > 7 \text{ nm}$, the gaps of the FQHE states in the $n = 0$ and $n = 1$ Landau levels become comparable. Experimental observation of these theoretical predictions, just as in the case of graphene [7–9], would be an important advancement in understanding the nature of correlated Dirac fermions in this unique state of matter.

The work has been supported by the Canada Research Chairs Program of the Government of Canada.

-
- [†] Electronic address: tapash@physics.umanitoba.ca
- [2] K.S. Novoselov, Rev. Mod. Phys. **83**, 837 (2011); A.K. Geim, *ibid.* **83**, 851 (2011).
- [3] D.S.L. Abergel, V. Apalkov, J. Berashevich, K. Ziegler, and T. Chakraborty, Adv. Phys. **59**, 261 (2010).
- [4] J.W. McClure, Phys. Rev. **104**, 666 (1956); R.R. Haering and P.R. Wallace, J. Phys. Chem. Solids **3**, 253 (1957); H. Sato, J. Phys. Soc. Jpn. **14**, 609 (1959).
- [5] Z. Jiang, et al., Phys. Rev. Lett. **98**, 197403 (2007).
- [6] Y. Zhang, et al., Phys. Rev. Lett. **96**, 136806 (2006).
- [7] V.M. Apalkov and T. Chakraborty, Phys. Rev. Lett. **97**, 126801 (2006), see also, N. Shibata and K. Nomura, J. of Phys. Soc. Jpn. **78**, 104708 (2009).
- [8] D.A. Abanin, et al., Phys. Rev. B **81**, 115410 (2010).
- [9] F. Ghahari, et al., Phys. Rev. Lett. **106**, 046801 (2011).
- [10] P.R. Wallace, Phys. Rev. **71**, 622 (1947).
- [11] M.Z. Hasan and C.L. Kane, Rev. Mod. Phys. **82**, 3045 (2010).
- [12] X.-L. Qi and S.-C. Zhang, Phys. Today **63**, 33 (2010).
- [13] There are several ways the Dirac surface state of a TI differs from the Dirac cones in graphene. In the TI, a single Dirac cone can form in the surface Brillouin zone, while in graphene they always come in pairs. The Dirac cone of TI is robust against any time-reversal invariant perturbations. Dirac cones in graphene have spin degeneracy which is absent in the TI [14].
- [14] T. Hanaguri, et al., Phys. Rev. B **82**, 081305 (R) (2010).
- [15] P. Cheng, et al., Phys. Rev. Lett. **105**, 076801 (2010).
- [16] T. Chakraborty and P. Pietiläinen, *The Quantum Hall Effects* (Springer, New York 1995) 2nd. edition.
- [17] C.-X. Liu, et al., Phys. Rev. B **82**, 045122 (2010).
- [18] H. Zhang, et al., Nat. Phys. **5**, 438 (2009).
- [19] Z. Wang, et al., Phys. Rev. B **82**, 085429 (2010).
- [20] Z. Yang and J.H. Han, Phys. Rev. B **83**, 045415 (2011)
- [21] F.D.M. Haldane, Phys. Rev. Lett. **51**, 605 (1983).